buildings

Article

Determination of the Target Reliability Index of the Concrete Main Girder of Long-Span Structures Based on Structural Design Service Life

Zhenhao Zhang [1,2], Hesheng Li [1], Jun Xiong [1], Fuming Wang [1,2], Leijun Wei [1] and Lu Ke [2,3,*]

[1] School of Civil Engineering, Changsha University of Science and Technology, Changsha 410114, China
[2] Guangxi Key Laboratory of Disaster Prevention and Engineering Safety, Guangxi University, Nanning 530004, China
[3] College of Civil Engineering and Architecture, Guangxi University, Nanning 530004, China
* Correspondence: chinakexue@126.com

Abstract: This article studies the quantitative relationship between the target reliability index and the design service life for concrete main girders of cable-stayed bridges. A resistance degradation model of the concrete components is established by quantifying the effects of concrete carbonation and steel corrosion. It is assumed that the dead load and the live load are time-invariant with the distributions of normal and extreme type I, respectively, while the resistance is considered as time-variant with the distribution of lognormal. The standard values of the most unfavorable moment under dead and live loads are calculated by ANSYS, its mean value and standard deviation are further obtained using the statistical parameters suggested by the Unified Standard for Structural Reliability Design of Highway Engineering. The mean and standard deviation of resistance are obtained using the target reliability index value provided in the code above. The resistance value and reliability index at different times in a certain design service life can be obtained through the resistance degradation model. The result shows the reliability index decreases exponentially during the service life of the structure. For different design service years, different initial resistance values and initial reliability indexes can be deduced. Based on this, the target reliability index values considering the design service life are suggested. In the example analysis, the target reliability index of the concrete main girder of a cable-stayed bridge with a design service life of 100 years is suggested as 6.24. This research provides references for the design of concrete main girders of cable-stayed bridges.

Keywords: long-span concrete girder; target reliability index; design service life; concrete carbonation; steel corrosion

Citation: Zhang, Z.; Li, H.; Xiong, J.; Wang, F.; Wei, L.; Ke, L. Determination of the Target Reliability Index of the Concrete Main Girder of Long-Span Structures Based on Structural Design Service Life. *Buildings* **2022**, *12*, 2249. https://doi.org/10.3390/buildings12122249

Academic Editors: Mohamed K. Ismail, Oldrich Sucharda, Ahmed Senouci and Flavio Stochino

Received: 9 November 2022
Accepted: 14 December 2022
Published: 16 December 2022

1. Introduction

With the increasing of service life of bridges, the carbonation of concrete and the corrosion of steel bars will lead to the deterioration of bridges and even pose a safety hazard to bridges [1–7]. For long-span cable-stayed bridges, the design reference period is generally 100 years in China [8], so it is unreasonable to carry out major repair in 20–30 years or so [9,10]. To ensure an adequate service life, it is important to scientifically select the target reliability index values of the key components of cable-stayed bridges.

At present, most research has focused on the target reliability index of medium- or small-span bridges, while the studies on long-span bridges (including cable-stayed bridges) are fewer. The calibration method is traditionally used to study the target reliability index. This method has been used to study the target reliability index of medium- and small-span highway reinforced concrete beam bridges and railway steel bridges [11–15]. The recommended target reliability index basically corresponds to the current unified standard of reliable design in China. The essence of the calibration method is to obtain the implied reliability level from the current code by back-analysis and then determine the target reliability index on it. In other words, the calibration method must be based on a given code. Obviously, this is not suitable for long-span cable-stayed bridges. In fact, studies on the target reliability index of the small and medium span are not perfect either. For example, for prestressed concrete members whose design is controlled by serviceability limit states, the existing codes have not provided the target reliability index for crack resistance, deflection, and stress [16]. The research on the target reliability index of long-span cable-stayed bridges is even sparser. Zhang et al. studied the reasonable value of the target reliability index of the steel main girder of cable-stayed bridge considering durability [17–19].

Ang et al. and Zhu et al. proposed an approach for obtaining the optimal target reliabilities (or acceptable risks) for damage control and collapse prevention of reinforced concrete buildings against earthquake hazards [20–22]. However, this work was not for the long-span bridges. Nowak and Kaszynska studied the target reliability index of girder bridges under ultimate limit states and serviceability limit states [23]. The calibration method was used on the previous AASHTO LRFD bridge design specifications (1998). This work also targeted medium- and small-span bridges. Lee et al. studied the target reliability index of a long-span cable-supported bridge (LSCSB) in Korea [24]. A concept to differentiate the target reliability for the design of an LSCSB was suggested and the target reliability was determined according to the importance of a structure. However, this work only presented the target reliability index for the cable elements of LSCSBs. Although cable-stayed bridge construction has been widely used in the past decade, statistical data are scarce. In addition, due to the lack of relevant design specifications, there are few studies on the target reliability index of a cable-stayed bridge structure.

Within the last two decades, many scholars have comprehensively considered different factors to determine the target reliability index of structures. For example, Wen took into account the uncertainty of the loading process and structural response for buildings in the new structure's design and existing structure's evaluation, and minimized the expected lifetime cost to determine the corresponding target reliability index [25]; Katade and Katsuki proposed to determine the target reliability index of structures based on the trade-off between the probability of failure and structural cost [26]; Huaco et al. considered the socially acceptable risk and economic concerns to define the target reliability index [27]; Holicky regarded construction cost, failure consequences, design life, and discount rate as characteristic parameters, trying to find out the influence of characteristic parameters on the target reliability index of structures [28]; Yanaka et al. analyzed the target reliability index of prestressed girders of bridges subjected to corrosion conditions under considering the optimization of the initial, maintenance, and failure costs [29]; Ghasemi and Nowak established an optimization procedure to determine the target reliability index of structures with consideration of the construction cost, failure cost, maintenance cost, structural lifetime, discount rate, time-dependency of the load and resistance, and structural importance factors [30]. These studies determine target reliability index based on the perspective of structural life-cycle costs. Kim et al. presented a novel probabilistic approach to determine the target reliability index of an individual bridge at the bridge network level [31]. The target reliability index of a bridge is determined according to the structural importance indicator of the bridge in a network. This research moves the research perspective from an individual bridge to the bridge network. The optimization for the reliability index in the above research requires the minimum threshold level of the reliability index to be known, while the target reliability index in the design codes and standards is the recommended reliability level to be kept annually. Therefore, it is essential to figure out the variation law of the target reliability index of structures within the design service life. Nguyen et al. presented a probabilistic model and approach to formulate and analyze the reliability-based design optimization of prestressed concrete box girder bridges with consideration of the pitting corrosion phenomenon of shear, torsion reinforcements, and post-tensioned tendon, while this study only posed the target reliability index range for the simple support prestressed concrete box girder bridges [32].

In summary, the research on the influence factors, reasonable values of target reliability index, and its determination methods is sufficient for small- and medium-span structures, but currently there is little such work on that of the complex large-scale structures, including long-span cable-stayed bridges. In order to discuss and provide a reasonable value of the target reliability index of the cable-stayed bridge, this paper studies the deterioration law of the resistance of the concrete main girder of the cable-stayed bridge with the increase in the service life considering concrete carbonation and steel corrosion. Then, based on the quantitative relationship between the design service life and the target reliability index of the structure, a reasonable value of the target reliability index for the concrete main girder of the long-span cable-stayed bridges is presented. The research results will provide a theoretical reference for the design, operation, and maintenance of concrete cable-stayed bridges.

2. Statistical Analysis of Load and Resistance

2.1. Statistical Analysis of Load

2.1.1. Statistical Analysis of Dead Load

The dead load can be approximated as a constant during the design reference period, so the random variable probability model is used to describe it. Existing studies have conducted surveys on a dead load of reinforced concrete and prestressed concrete bridges. The actual measurement includes the self-weight of reinforced concrete, prestressed concrete T-beams, box beams and slabs, and the unit weight and thickness of asphalt concrete and cement concrete on the bridge deck. Through analysis of the measured data, the dead load does not reject the normal distribution. A dead load of a bridge is composed of component weight and bridge deck weight, combining their statistical parameters, taking the bridge deck weight as 10%, 15%, 20%, 25%, and 30% of the total weight of the structure for a combination. Analysis shows that the different ratios between bridge deck weight and component weight have little effect on the statistical parameters of the dead load. The combined statistical parameter distribution type is still normal distribution and can be taken as

$$K_G = \mu_{\mathrm{G}/} G_{\mathrm{k}} = 1.0148$$

$$\delta_{\mathrm{G}} = 0.0431$$

where μ_G is the mean value of the measured component weight or bridge deck weight. G_k is the component standard weight or bridge deck standard value specified in the current code (i.e., the standard unit weight multiplied by the design volume). δ_G is the coefficient of variation of statistical parameters [33].

2.1.2. Statistical Analysis of Vehicle Load

The vehicle load varies depending on some factors such as traffic flow, geographic area, and grade of the bridge, and the distribution of the lane load must satisfy the requirements of the specification [34]. Using the Road Vehicle Dynamic Tester, the vehicle load is investigated. Measurement points are set up on some representative highways, and then the continuously measured data of the natural fleet are removed, and the abnormal values are selected as the vehicle load samples. In the statistical analysis of the vehicle load, dense traffic state and general traffic state are considered. The former represents a state in which the time interval between two adjacent vehicles is less than 3 s, and also includes a traffic jam state, and the latter represents a state in which the time interval between two adjacent vehicles is 3 s or more. Finally, on the basis of vehicle load investigation and analysis, various types of vehicle load effects with control functions are obtained through a large number of calculations for different bridge types and various spans. Obviously, different vehicle load effects (e.g., moment, shear) have different statistical parameters.

The calculation of the vehicle load effect also contains general and dense traffic states for statistical analysis, and the dimensionless parameter is also used in its reliability analysis,

$$K_{SQ} = S_Q/S_{QK} \tag{1}$$

where S_Q is the calculated effect value of the vehicle load, divided into general and dense traffic states, and S_{QK} is the nominal value of the vehicle load specified in the current code [33].

2.2. Time-Varying Model of Resistance Degradation

2.2.1. General Trend of Resistance Degradation

In a reinforced concrete structure, the steel bar starts to rust when carbonation reaches a certain depth. Therefore, it is considered that there is no corrosion on the surface of the steel bar from the beginning of service to a certain time t_c.

The effect of concrete carbonation on a structure is to decrease the stress area, damage the sectional size, and reduce the bearing capacity. Darmawan et al. set up statistical parameters of concrete cube compressive strength that change with time [35]. Enright et al. analyzed the data of existing bridges and corrected the result of the analyses [36]. It was concluded that the strength of the concrete will increase with time. In new bridges, the design of concrete mix to fulfil certain durability requirements would prevent the onset of the carbonation process. The increase in the compressive strength of concrete after 2 to 5 years of service is very small and can be safely assumed to be constant.

At time t_c, the corrosion occurring with carbonation reaches the surface of steel bars. The resistance degradation of the structural members becomes relatively large because the concrete carbonation and the steel bar corrosion causes the concrete section size and the reinforcement section area to decrease. In addition, the material properties of the members will degrade over time, as shown in Figure 1.

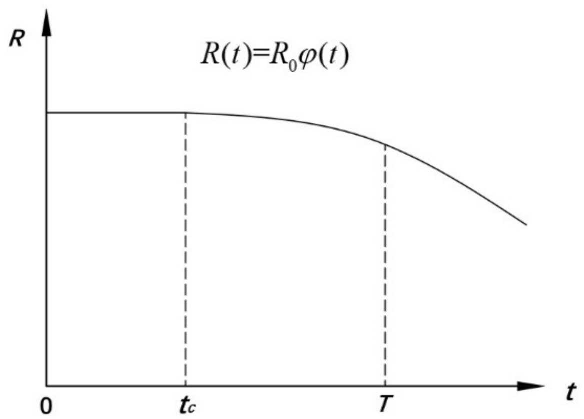

Figure 1. Schematic diagram of resistance vs. time.

In recent years, many scholars have studied the resistance degradation model and obtained many different models [37–46]. However, the expressions of these models are basically the same, as they adopt a degradation function of the initial resistance of the structure multiplied by a coefficient less than 1, as shown below:

$$R(t) = R_0\varphi(t) \tag{2}$$

where R_0 is the initial resistance of the structure member at time t = 0, and $\varphi(t)$ is the resistance degradation function [47].

2.2.2. A Time-Varying Resistance Model Considering the Concrete carbonation and Steel-Bar Corrosion

This section mainly considers the impact of concrete carbonation and steel bar corrosion on the reinforced concrete main girder of cable-stayed bridges and establishes a resistance degradation model by the coefficient of section loss of the member. The structures are in a natural environment. Sarja and Vesikari studied the resistance degradation function of reinforced concrete flexural members in a natural environment and gave it the form

$$\varphi(t) = \begin{cases} 1 \; 0 \leq t \leq t_c \\ 1-\lambda = 1-\omega(t-t_c) \; t_c \leq t \leq T \end{cases} \tag{3}$$

where ω is the coefficient of section loss of the member, and t_c is the duration of carbonation reaching the surface of the steel bar, ignoring the effects of carbonation residue [48].

- Initial Time of Steel-bar Corrosion

According to the theoretical analysis and experiments, in a general atmospheric environment, the formula of the initial time for steel-bar corrosion is

$$t_c = \left(\frac{c}{K}\right)^2 \tag{4}$$

where c is the concrete cover depth (40 mm), and K is the coefficient of concrete carbonation, which has the form

$$K = K_{el} K_{ei} K_t \left[\frac{24.48}{\sqrt{f_{cu}}} - 2.74\right] \tag{5}$$

where K_{el} is a local coefficient (1.0 in the north, and 0.5–0.8 in the south and foreland) because the impact of freeze-thaw and deicing salts should be considered in northern China, while the impact of freeze-thaw and deicing salts is less considered in the southern region, and the air humidity in the south is greater than the north, K_{ei} is an indoor and outdoor coefficient (1.87 inside and 1.0 outside), K_t is the coefficient of concrete curing time (1.50 in general construction), and f_{cu} is the cubic concrete compressive strength (C50) [49–51].

Through the calculation according to Equations (4) and (5), t_c can be obtained as 14 years.

- Ratio of Concrete Section Loss

In the natural environment, steel-bar corrosion can be considered to start when the concrete carbonation in reinforced concrete reaches its surface. According to this principle, the prediction model of concrete carbonation depth is generally accepted as

$$D(t) = K\sqrt{t} \tag{6}$$

where D is carbonation depth, t is carbonation duration, and K is the carbonation coefficient [52,53].

Concrete carbonation results in the reduction of section size. A box girder is used as the research object in this paper, and a simplified box section is considered, as shown in Figure 2 (h'_f is the height of compression flange, h is the height of section, h_f is the height of tension flange, d is the thickness of web, and b is the width of section).

The reduction coefficients of the section sizes b and h of the structural member are [54]

$$\alpha(b,t) = \frac{[b(0) - 2D(t)]}{b(0)} = 1 - \frac{2K\sqrt{t}}{b(0)} \tag{7}$$

$$\alpha(h,t) = \frac{[h(0) - 2D(t)]}{h(0)} = 1 - \frac{2K\sqrt{t}}{h(0)} \tag{8}$$

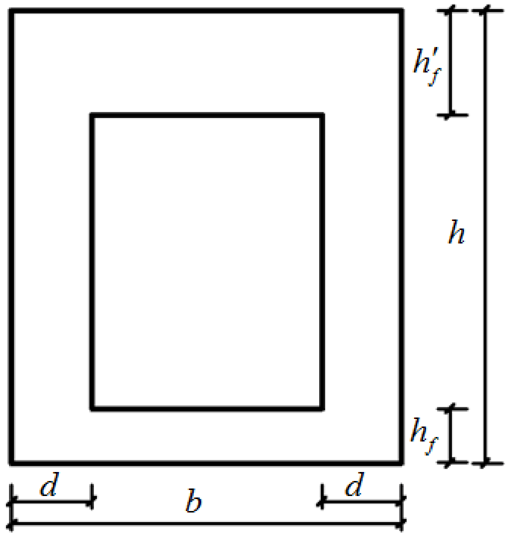

Figure 2. Box section model.

The time-varying side length of the member is

$$b(t) = \alpha(b,t) \cdot b(0) \quad (9)$$

$$h(t) = \alpha(h,t) \cdot h(0) \quad (10)$$

The ratio of concrete section loss is

$$\omega_1 = \frac{b(0)h(0) - b(t)h(t)}{b(0)h(0)} = 1 - \alpha(b,t)\alpha(h,t) = 0.001001\sqrt{t} - 0.0000964t \quad (11)$$

- Ratio of Steel-Bar Section Loss

The area of corroded steel-bar is

$$A(t) = \alpha(A,t) \cdot A(0) \quad (12)$$

where *A(0)* is the initial maximum area of longitudinal reinforcement, and $\alpha(A,t)$ is the reduction coefficient of the steel area caused by corrosion,

$$\alpha(A,t) = 1 - \lambda(t) \cdot t \quad (13)$$

where $\lambda(t)$ is the section loss ratio of the corroded steel bar, which can be obtained by the width of the corrosion crack [55]. The equation is

$$\lambda(t) = 0.01\beta_1\beta_2\beta_3\left(\frac{4.18}{f_{cu}} - 0.073\right)(1.85 - 0.04c)\left(\frac{5.18}{d} + 0.13\right)(t - t_c) \quad (14)$$

where β_1 is the curing coefficient of formed concrete under standard conditions, which is taken as 1.0; β_2 is the influence coefficient of the cement variety (1.7 for slag cement, 1.0 for P.O.); β_3 is the coefficient of the local environment which varies by region and is usually taken as 1.0; c is the concrete cover depth; and *d* is the diameter of the steel-bar.

The ratio of steel-bar section loss is

$$\omega_2 \frac{A(0) - A(t)}{A(0)} = 1 - \alpha(A,t) = 0.000000272(t - 14) \times t \quad (15)$$

Before the corrosion, the resistance can be considered unchanged, i.e., ω_2 = 0 and $\varphi(t)$ = 1 in the period [0, 14]. In the time segment [14, T], the structure's resistance has been reduced where corrosion occurs. In addition, the resistance degradation is affected by both concrete carbonation and steel-bar corrosion. Hence, the coefficient of section loss is $\omega = \omega_1 + \omega_2$, and the function of resistance degradation of the structural member can be obtained as

$$\varphi(t) = \begin{cases} 1 & 0 \le t \le 14 \\ 1 - \omega(t-14) & 14 \le t \le T \end{cases} \tag{16}$$

where

$$\omega = \omega_1 + \omega_2 = 0.001001\sqrt{t} - 0.0000964t + 0.000000272(t-14) \times t \tag{17}$$

3. Reasonable Selection of the Target Reliability Index of the Long-Span Main Girder

3.1. Analysis Flow of Relationship between Service Life and Target Reliability Index

For the main girder of a long-span cable bridge, it is assumed that the dead load and live load are time invariant while the resistance decreases with time; and the dead load is normally distributed, the live load follows an extreme type I distribution, and the resistance is lognormal distributed. The time-varying limit state equation is established as below:

$$Z(t) = R(t) - G - Q \tag{18}$$

where $R(t)$ is the time-variant structural resistance; G is the dead load; and Q is the vehicle load.

Based on the model of resistance degradation considering concrete carbonation and steel corrosion, a reliability index that can be calculated by the first-order reliability method, and the steps of calculating and analyzing the target reliability index of a concrete girder of a cable-stayed bridge can be obtained as follows:

1. calculate the standard values of the dead load, and vehicle load of the main girder;
2. obtain the mean, standard deviation, and coefficient of variation of dead load, vehicle load, and resistance from the *Unified Standard for Structural Reliability Design of Highway Engineering* [33];
3. calculate the reasonable resistance at the end of the design service life according to the recommended reliability index;
4. calculate the resistance deterioration $\varphi(t)$ at different times according to the resistance degradation model;
5. correct the standard and mean value of resistance according to the resistance deterioration;
6. calculate the reliability index at different times by the first-order reliability method;
7. calculate the suggested value of the initial reliability index under different service life, and then obtain a quantitative relationship between the design service life and the target reliability index.

3.2. Analysis of Internal Force and Resistance of Main Girder of Cable-Stayed Bridge

3.2.1. General Engineering Situation

The structure of a long-span cable-stayed bridge with double cable planes uses a concrete beam with a length of 708 m and a span arrangement of 174 m + 360 m + 174 m. In addition, self-gravity is considered in the dead load; and the vehicle load is considered in the live load.

- Material Properties

For the main girder and cable tower, $E = 3.5 \times 10^{10}$ kN/m^2, $\rho = 2600$ kg/m^3, $\mu = 0.17$; for the cross-beams connecting the main towers and rigid fishbone cross-beam, $E = 1.0 \times 10^{16}$ kN/m^2, $\rho = 0$, $\mu = 0$; for the stayed-cable, $E = 1.9 \times 10^{11}$ kN/m^2, $\rho = 1200$ kg/m^3, $\mu = 0.27$.

- Geometric Property of Section

For the main girder, $a = 16$ m, $b = 1.6$ m, $A = 25.6$ m^2, $I_y = 2000$ m^4, $I_z = 20$ m^4, $I_x = 21.8$ m^4; for the cross-beams in the cable tower and the rigid fishbone beams, $a = 1$ m, $b = 1$ m, $A = 1$ m^2, $I_y = 1/12$ m^4, $I_z = 1/12$ m^4, $I_x = 1/3$ m^4; for the stayed-cable, $A = 0.72$ m^2.

- Structural Size

The width of the bridge is 28 m; the height of the tower is 162 m; the length of the crossing-girder joining the main towers is 30 m; the distance from the bridge deck to the bifurcation point of the inverted *Y* is 60 m; the distance from the bottom of the bridge tower to the bridge deck is 30 m; and the lateral distance of the tower's bottom is 20 m, as shown in Figure 3.

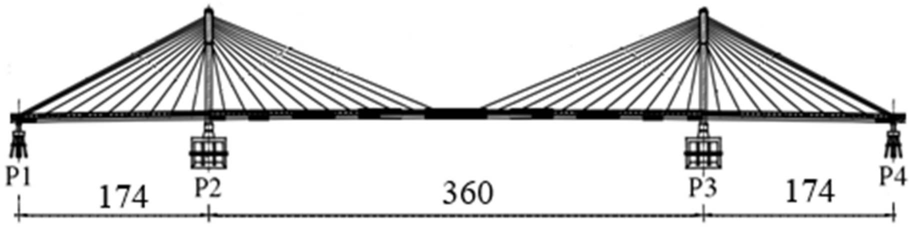

Figure 3. Structural size of the bridge.

3.2.2. ANSYS Model and Results of Finite Element Analysis

ANSYS was used to establish the special fishbone model. It is considered that all the mass of the cable-stayed bridge is concentrated on the main girder and that the cross-beams are rigid components without weight and only act as passing-force components. Other model and analysis assumptions are as follows.

1. The main girder of the cable-stayed bridge is completely floating, and at the end of the cable tower and the cable-stayed bridge, the main girder releases longitudinal constraints.
2. The middle- and lower-tower columns are simulated by the same beam element, while the upper-tower column is simulated by four beam elements and the cable-tower beam by two rigid beam elements.
3. According to *General Specifications for Design of Highway Bridge and Culverts* (JTG D60-2015, Beijing China), use the Road-I level load as the live load, which contains a uniform load with the value of 10.5 kN/m and a concentrated load with the value of 360 kN. Considering the most dangerous internal force of mid-span section (control section generally), the uniform load is fully distributed between the two towers, and the concentrated load is located at the mid-span position.
4. Boundary conditions: Freedom constraints are imposed in both the vertical and lateral directions on the left end of the bridge, and for the rigid cross-beams on the main girder of the cable tower on the right end of the bridge, they are imposed on the right end of the bridge in the lateral direction and on the bottom of the cable tower, and complete hinge constraints are imposed on all cable and beam elements.

The calculation results of the finite element model under dead and live loads are as below.

1. Under the dead load, the most unfavorable displacement of the main girder in the middle of the span is D_G = 0.1197 m, and the most favorable moment is M_G = 22,200 kN·m, as shown in Figures 4 and 5.
2. Under the vehicle load, the most unfavorable displacement of the main girder of a cable-stayed bridge is D_Q = 0.0079 m, and the largest bending moment is M_Q = 2200 kN·m, as shown in Figures 6 and 7.

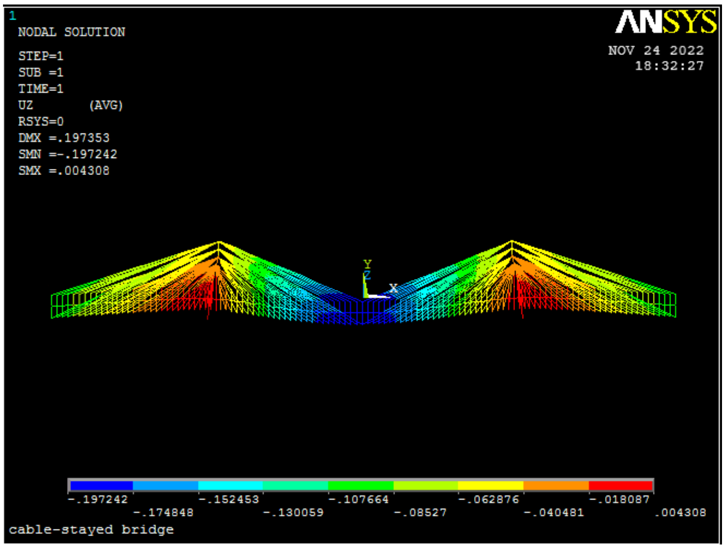

Figure 4. Deformation of main girder of cable-stayed bridge under dead load.

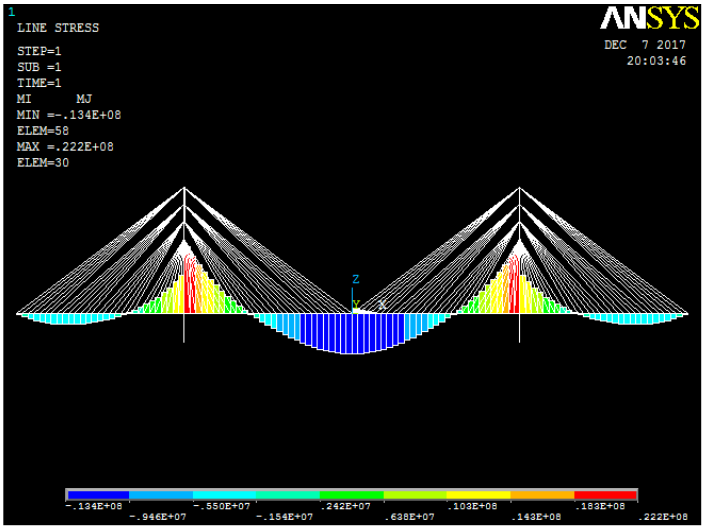

Figure 5. Bending moment distribution of main girder of cable-stayed bridge under dead load.

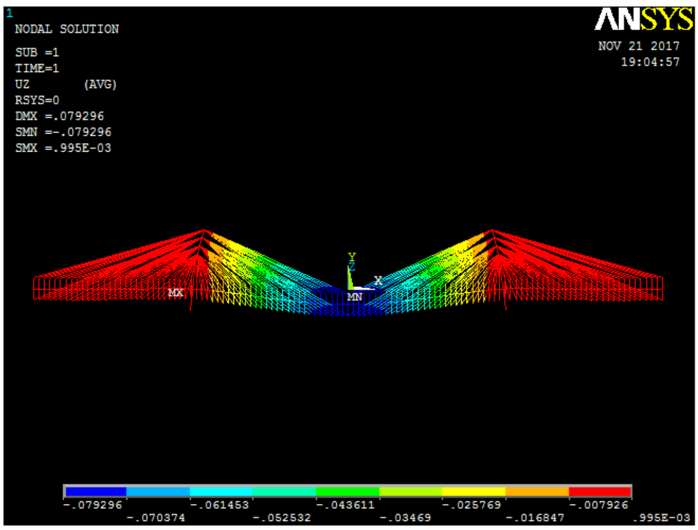

Figure 6. Deformation of main girder of cable-stayed bridge under vehicle load.

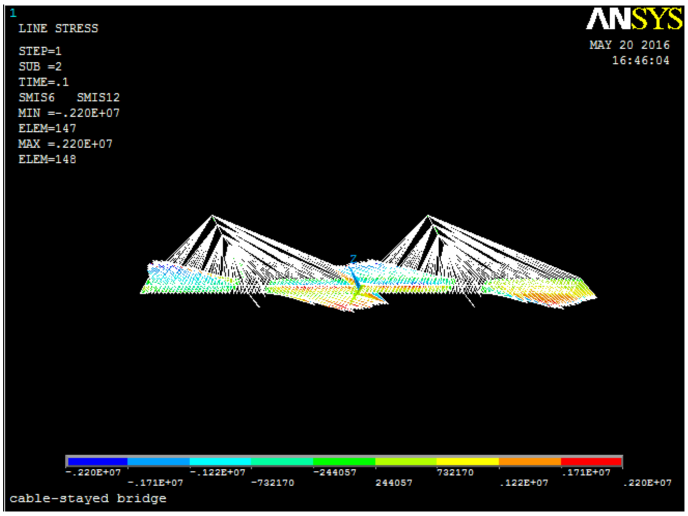

Figure 7. Bending moment distribution of main girder of cable-stayed bridge under vehicle load.

3.2.3. Parametric Statistics

- Parametric Statistics of Dead Load

The mean, standard deviation, and coefficient of variation of the main girder of a long-span cable-stayed bridge under a dead load are, respectively

$$\mu_G = 1.0148M_G = 1.0148 \times 22,200 = 22,528.6 \text{ kN} \cdot \text{m}$$

$$\sigma_G = 0.4374M_G = 0.4374 \times 22,200 = 971 \text{ kN} \cdot \text{m}$$

$$\delta = 0.0431$$

- Parametric Statistics of Live Load

The maximum value of the vehicle load effect depends on the distribution of the maximum value in the design working life, which obeys an extreme I distribution.

The mean and standard deviation can be obtained from the parametric statistics of the vehicle load [33].

The mean and standard deviation in general traffic state are

$$\mu_{Q1} = 0.686M_G = 0.686 \times 2220 = 1522.9 \text{ kN} \cdot \text{m}$$

$$\sigma_{Q1} = 0.1098M_Q = 0.1098 \times 2220 = 243.76 \text{ kN} \cdot \text{m}$$

The mean and standard deviation in dense traffic state are

$$\mu_{Q2} = 0.7995M_Q = 0.7995 \times 2220 = 1774.9 \text{ kN} \cdot \text{m}$$

$$\sigma_{Q2} = 0.0719M_Q = 0.0719 \times 2220 = 159.6 \text{ kN} \cdot \text{m}$$

In a practical situation, it can be assumed that the bridge is under a dense traffic state at 10 percent of its service time, and at other times it is under a general traffic state. Therefore, the mean value, standard deviation, and coefficient of variation can be calculated as

$$\mu_Q = 90\% \times \mu_{Q1} + 10\% \times \mu_{Q2} = 1534.5 \text{ kN} \cdot \text{m}$$

$$\sigma_Q = \sqrt{(90\% \times \sigma_{Q1})^2 + (10\% \times \sigma_{Q2})^2} = 218 \text{ kN} \cdot \text{m}$$

$$\sigma = 0.142$$

- Resistance Parameters

The *Unified Standard for Structural Reliability Design of Highway Engineering* (Industry Standards of the People's Republic of China) [8] requires carrying out ultimate limit states design of bearing capacity under persistent design situations, the target reliability index of components in highway bridge should not be less than 4.7. This target reliability index comes from calibration methods and mature engineering experience, and the current structural design complies with this requirement. This means that in the case of determining the load effect, the reasonable design value of the resistance of the member can be estimated if the coefficient of variation of the resistance statistics is known.

There are many factors that affect the resistance of structural members, but the following three are usually considered: the uncertainty of material properties, the uncertainty of structural geometric parameters, and the uncertainty of calculation modes. Collecting and analyzing their statistical parameters, the resistance statistical parameters of different components can be calculated by using the resistance calculation formula and the error propagation formula. Existing studies have shown that for reinforced concrete members subjected to bending at the normal section, the statistical parameters of the resistance are [33]

$$K_R = \frac{\mu_R}{R_k} = 1.2262$$

$$\delta_R = 0.1414$$

where R_k is the resistance value of the member obtained by the resistance calculation formula according to the standard values of material properties and geometric parameters; μ_R is the mean value of resistance; δ_R is the coefficient of variation of resistance.

Knowing μ_G, σ_G, μ_Q, σ_Q, and δ_R and taking the target reliability index β_T as 4.7, μ_R can be calculated. Select the initial value of μ_R, calculate the reliability by the JC method, compare it with 4.7 and through repeated iterations, the value of μ_R is finally obtained. The iteration termination condition is $4.7 < \beta < 4.71$. The calculation results are as follows.

$$\beta = 4.7058$$

$$\mu_R = 48{,}316 \text{ kN} \cdot \text{m}$$

$$\sigma_R = \delta_R \cdot \mu_R = 6831.9 \text{ kN} \cdot \text{m}$$

3.3. Calculation Results of Target Reliability Index

μ_R and σ_R calculated above are used to be the statistical parameter of the resistance of the main beam after servicing 100 years, which ensures that the reliability index of the main beam after servicing 100 years is not less than 4.7. Then, through Equations (2) and (16) and assuming that δ_R remains unchanged, the resistance and reliability index of the component from 0 to 100 years can be calculated. MATLAB is used to calculate the time-varying reliability index. The results are shown in Table 1.

Table 1. Time-varying reliability index $\beta(t)$ and its attenuation $\Delta\beta(t)$ of main girder of cable-stayed bridge.

t	14	20	30	40	50	60	70	80	90	100
$\varphi(t)$	1	0.997	0.995	0.990	0.980	0.964	0.939	0.904	0.858	0.799
$\beta(t)$	6.2425	6.2219	6.2082	6.1736	6.1041	5.9913	5.8113	5.5512	5.1935	4.7058
$\Delta\beta(t)$	0	0.0206	0.0343	0.0689	0.1384	0.2512	0.4312	0.6913	1.0490	1.5367

Note: t is the service life, $\varphi(t)$ is the resistance degradation values.

According to the data in Table 1, the expression of the time-dependent reliability index can be obtained using the Origin software for exponential function fitting,

$$\beta(t) = 6.31379 - 0.03294e^{\frac{t}{25.65951}} \tag{19}$$

The fitting curve for the reliability index $\beta(t)$ is shown in Figure 8.

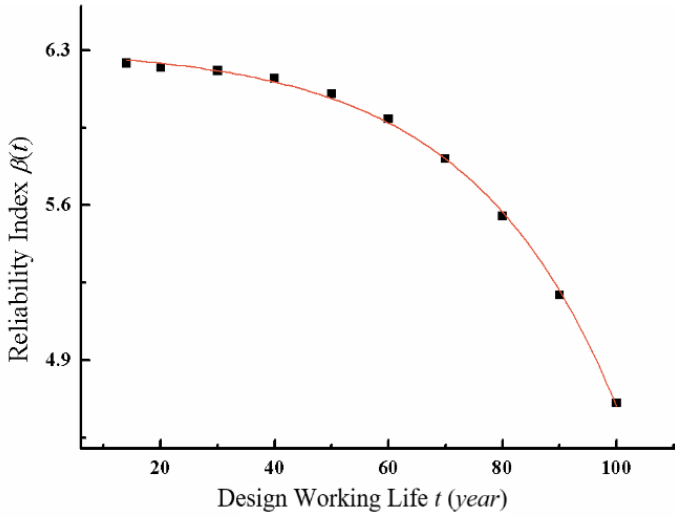

Figure 8. Time-varying reliability index of main girder of cable-stayed bridge.

The exponential function is also used to fit the data of the reliability index attenuation $\Delta\beta(t)$ in Table 1, and the expression is obtained as

$$\Delta\beta(t) = -0.07129 + 0.03294e^{\frac{t}{25.65952}} \tag{20}$$

The fitting curve for the reliability index attenuation $\Delta\beta(t)$ is shown in Figure 9.

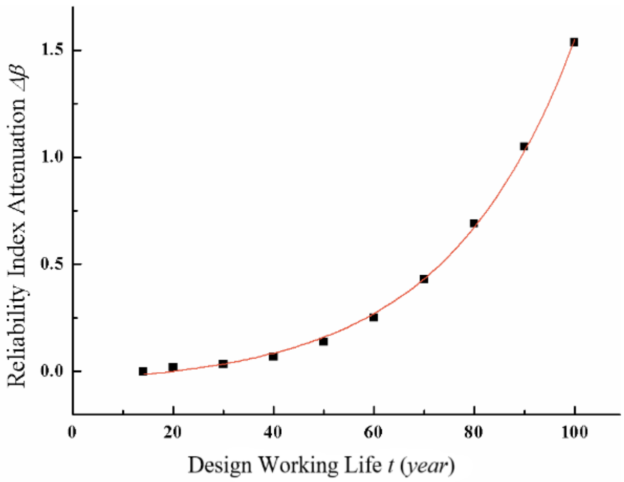

Figure 9. Reliability index degradation of main girder of cable-stayed bridge.

From the calculation results above, it can be obtained that

1. Based on the resistance model concerning concrete carbonation and steel corrosion, the degradation curve of the reliability index changes slowly.
2. Before carbonation reaches the steel surface, the structural reliability index is almost constant. The later the steel bar starts to rust, the better the structural reliability. The initial time of steel bars corrosion is closely related to the local environment. Thus, even if the steel bars have already started to rust, as long as the micro-environment of the main girder is under control, its structural load carrying capacity can be guaranteed.

3.4. Relationship between Target Reliability Index and Service Life

For a structure with a design service life of 100 years, the target reliability index is suggested to be 4.7 in ultimate limit states. The design service life and target reliability index β_T are interconnected, and according to the dynamic reliability analysis of the main girder in a previous paper, it can be obtained that the reliability index decreases with the service time, and therefore, it is necessary to adjust the target reliability index to ensure the reliability of the structure during the whole service life [56]. Additionally, the adjustment range is related to the degree of resistance degradation and the design working life.

In the same way as above, take μ_R and σ_R as the statistical parameters of the resistance of the main girders after servicing 90, 80, 70, 60, 50, 40, 30, and 20 years, then the time-varying reliability can be obtained. The results shown in Table 2 and Figure 10 pose the decay process of different initial reliability during the corresponding service life. Experiencing the corresponding service life, the initial reliability indexes become about 4.7. In other words, these initial reliability indexes are the target reliability indexes which ensure that the reliability index is still slightly greater than 4.7 when the component has gone through the corresponding service life.

Table 2. Time-varying reliability index $\beta(t)$ of cable-stayed bridge.

t	**14**	**20**	**30**	**40**	**50**	**60**	**70**	**80**	**90**
$\varphi(t)$	1	0.997	0.995	0.990	0.980	0.964	0.939	0.904	0.858
$\beta(t)$	5.7545	5.7339	5.7201	5.6856	5.6161	5.5033	5.3234	5.0633	4.7058
$\beta(t)$	5.3968	5.3762	5.3625	5.3280	5.2584	5.1457	4.9658	4.7058	/
$\beta(t)$	5.1367	5.1161	5.1024	5.0679	4.9984	4.8857	4.7058	/	/
$\beta(t)$	4.9568	4.9362	4.9225	4.8880	4.8185	4.7058	/	/	/
$\beta(t)$	4.8441	4.8235	4.8098	4.7753	4.7058	/	/	/	/
$\beta(t)$	4.7746	4.7540	4.7403	4.7058	/	/	/	/	/
$\beta(t)$	4.7401	4.7196	4.7058	/	/	/	/	/	/
$\beta(t)$	4.7264	4.7058	/	/	/	/	/	/	/

Note: t is the service life, $\varphi(t)$ is the resistance degradation values.

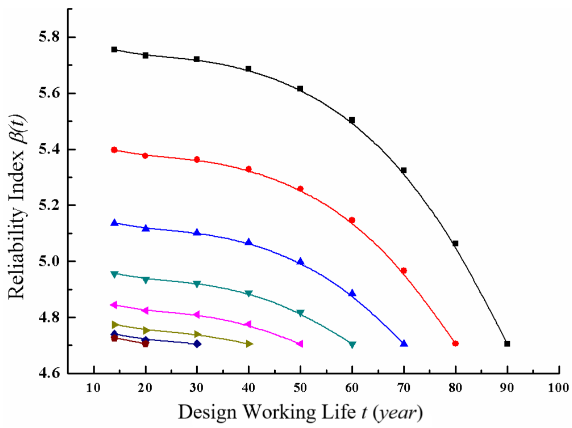

Figure 10. Time-varying reliability index of main girder of cable-stayed bridge with different initial reliability.

Different design service life and corresponding target reliability indexes are shown in Table 3. According to the data in Table 3, the expression of the target reliability index can be obtained by using the Origin software for exponential function fitting.

$$\beta_T = 4.63205 + 0.03339e^{\frac{t}{25.74022}} \tag{21}$$

Table 3. Relation between design service life and target reliability index.

t	**14**	**20**	**30**	**40**	**50**	**60**	**70**	**80**	**90**	**100**
β_T	4.7000	4.7264	4.7401	4.7746	4.8441	4.9568	5.1367	5.3968	5.7545	6.2425

The fitting curve of the target reliability index β_T is shown in Figure 11.

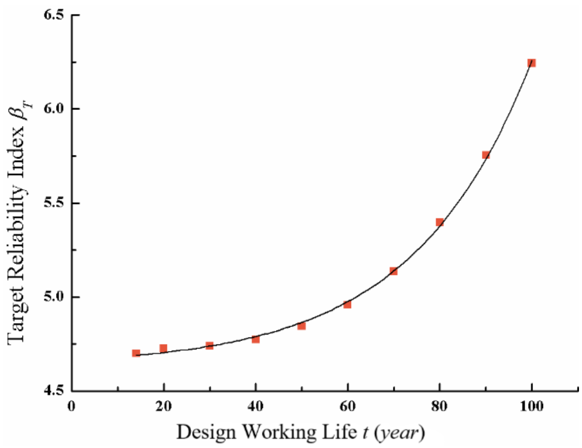

Figure 11. Relationship between target reliability index and design working life.

In summary, when resistance degradation caused by concrete carbonation and steel bar corrosion is considered, the target reliability index β_T based on the design working life can be set as

$$\beta_T = \begin{cases} 4.7 & 0 \leq t \leq 14 \\ 4.63205 + 0.03339 e^{\frac{t}{25.74022}} & 14 < t < T \end{cases} \tag{22}$$

3.5. Discussion

The above work constructs the method framework for the determination of target reliability indexes of cable-stayed bridge's main girder. Some simplified methods are used in the analysis process, which needs more discussion as below.

Regarding the most dangerous internal forces of the control section under vehicle load, the work in Section 3.2.2 only performs a rather approximate analysis. To be strict, the uniform load should be distributed fully on the influence line with the same sign and the concentrated load should be placed at the peak value position of the corresponding influence line. Further, for more accuracy, the vehicle load should be regarded as moving load and vehicle–bridge coupling vibration analysis should be implemented to obtain the most dangerous internal forces under random traffic flow. However, it can be thought that the simplified live load arrangement would have limited impact on the final reliability analysis results.

Regarding the applicability of this model, it should be pointed out that this function relation result is partly based on a specific cable-stayed bridge' force analysis, thus it would be applicable only for this specific cable-stayed bridge. A long-span cable-stayed bridge is complex large-scale infrastructure, whose reliability design should be constructed through case-by-case analysis, including the reasonable value of target reliability index and actually there is no specification to follow currently for long-span cable-stayed bridges.

Finally, it should be pointed out that this work considered the failure mode of bending, which is the main failure mode for a girder. For more comprehensive results, other failure modes of the main girder of cable-stayed bridges should be considered, but the target reliability index determination method will be the same as the one presented.

4. Conclusions

With the increasing of long-span bridges, the target reliability index for such bridges is attracting increasing attention. A reasonable value of the target reliability index can ensure the safety of the structure during its service life. Considering the concrete carbonation and steel corrosion in the natural environment, the quantitative relationship between the target reliability index and the design service life of the concrete main girder of a cable-stayed bridge was investigated, which can provide a scientific basis for the design of the concrete main beam of a long-span cable-stayed bridge.

1. Through the analysis using the resistance degradation model concerning concrete carbonation and steel corrosion, the reliability index of main girder of cable-stayed bridges decreases exponentially during the structural service life under the failure mode of bending.
2. A hybrid analysis framework composed of numerical method and analytical method is constructed for the cable-stayed bridge's target reliability index analysis, in which the most dangerous moment of the main girder under vehicle load is calculated by finite element analysis and the reliability index calculation is calculated by the first order second moment method.
3. The quantitative relationship between the target reliability index and the design service life was obtained as Equation (22). Based on that, the target reliability index of the concrete main girder of a cable-stayed bridge with a design service life of 100 years is suggested as 6.24, which is higher than the suggested values from the current relevant codes.

Author Contributions: Conceptualization, Z.Z.; methodology, Z.Z. and L.W.; software, F.W.; formal analysis, J.X. and L.W.; investigation, H.L.; writing—original draft preparation, H.L.; writing—review and editing, L.K. All authors have read and agreed to the published version of the manuscript.

Funding: This research was funded by [National Key R&D Program of China] grant number [2021YFB2600900], [Systematic Project of Guangxi Key Laboratory of Disaster Prevention and Engineering Safety] grant number [2021ZDK016], [Natural Science Foundation of Changsha City, China] grant number [kq2202210], and [Research Project of the Educational Commission of Hunan Province] grant number [22A0239, 20C0045]. The APC was funded by [Changsha University of Science and Technology].

Data Availability Statement: The data were included in the article.

Conflicts of Interest: The authors declare no conflict of interest.

References

1. Dan, M.F.; Strauss, A.; Kim, S. Bridge reliability assessment based on monitoring. *J. Bridge Eng.* **2008**, *13*, 258–270.
2. Pape, T.M.; Melchers, R.E. Performance of 45-year-old corroded prestressed concrete beams. *Struct. Build.* **2013**, *166*, 547–559. [CrossRef]
3. Frangopol, D.M.; Soliman, M. Life-cycle of structural systems: Recent achievements and future directions. *Struct. Infrastruct. Eng.* **2015**, *12*, 1–20. [CrossRef]
4. Frangopol, D.M.; Saydam, D.; Kim, S. Maintenance, management, life-cycle design and performance of structures and infrastructures: A brief review. *Struct. Infrastruct. Eng.* **2011**, *8*, 1–25. [CrossRef]
5. Sabatition, S.; Frangopol, D.M.; Dong, Y. Sustainability-informed maintenance optimization of highway bridges considering multi-attribute utility and risk attitude. *Eng. Struct.* **2015**, *102*, 310–321. [CrossRef]
6. Biondini, F.; Frangopol, D.M. Life-Cycle Performance of Deteriorating Structural Systems under Uncertainty: Review. *J. Struct. Eng.* **2016**, *142*, F4016001. [CrossRef]
7. Dong, D.M.F.Y.; Sabatino, S. Bridge life-cycle performance and cost: Analysis, prediction, optimisation and decision-making. *Struct. Infrastruct. Eng.* **2017**, *13*, 1–19.
8. Ministry of Transport of the People's Republic of China. People's Republic of China Industry Recommended Standard. In *Specifications for Design of Highway Cable-stayed Bridge*; JTG/T 3365-01—2020; Ministry of Transport of the People's Republic of China: Beijing, China, 2020.
9. Lee, J.Y.; Ellingwood, B.R. Ethical discounting for civil infrastructure decisions extending over multiple generations. *Struct. Saf.* **2015**, *57*, 43–52. [CrossRef]
10. Ellingwood, B.R.; Lee, J.Y. Life cycle performance goals for civil infrastructure: Intergenerational risk-informed decisions. *Struct. Infrastruct. Eng.* **2015**, *12*, 1–8. [CrossRef]
11. Li, G.; Cheng, G. Optimal decision for the target value of performance-based structural system reliability. *Struct. Multidiscip. Optim.* **2001**, *22*, 261–267. [CrossRef]
12. Suh, K.D. Evaluation of target reliability indices and partial safety factors for sliding of caisson breakwaters. *J. Coast. Res.* **2011**, *56*, 622–626.
13. Furuta, H. Bridge reliability experiences in Japan. *Eng. Struct.* **1998**, *20*, 972–978. [CrossRef]
14. Nowak, A.S. Calibration of LRFD Bridge Code. *ASCE J. Struct. Eng.* **1995**, *121*, 1245–1251. [CrossRef]
15. Nowak, A.S. *Calibration of LRFD Bridge Code*; NCHRP Report 368; Transportation Research Board: Washington, DC, USA, 1999.

16. American Association of State Highway and Transportation Officials. *AASHTO LRFD Bridge Design Specification*, 8th ed.; American Association of State Highway and Transportation Officials: Washington, DC, USA, 2017.
17. Zhang, Z.; Zhou, M.; Hu, C.; Liu, M. Research on Reasonable Value of Target Reliability Index for Steel Main Girder of Cable-Stayed Bridge Considering Durability. *Struct. Infrastruct. Eng.* **2019**, *15*, 1382–1391. [CrossRef]
18. Zhang, Z.; Zhou, M.; Fang, M. First-Passage Probability Analysis of Wiener Process using Different Methods and its Applications in the Evaluation of Structural Durability Degradation. *Eur. J. Environ. Civ. Eng.* **2019**, *25*, 1763–1781. [CrossRef]
19. Zhang, Z.; Li, W.; Yang, J. Analysis of Stochastic Process to Model Safety Risk in Construction Industry. *J. Civ. Eng. Manag.* **2021**, *27*, 87–99. [CrossRef]
20. Ang, A.H.-S.; Leon, D.D. Determination of optimal target reliabilities for design and upgrading of structures. *Struct. Saf.* **1997**, *19*, 91–103. [CrossRef]
21. Ang, A.H.-S.; Leon, D.D. Optimal target reliabilities for aseismic design of R/C buildings. In Proceedings of the Transactions of the 13th International Conference on Structural Mechanics in Reactor Technology, Porto Alegre, Brazil, 13–18 August 1995.
22. Zhu, B.; Frangopol, D.M. Risk-Based Approach for Optimum Maintenance of Bridges under Traffic and Earthquake Loads. *J. Struct. Eng.* **2013**, *139*, 422–434. [CrossRef]
23. Nowak, A.S.; Kaszynska, M. Target Safety Levels for Design and Evaluation of Bridges. *Trans. JWRI* **2003**, *32*, 189–196.
24. Lee, S.H.; Lee, H.H.; Paik, I.; Lee, H.S. Differentiation of Target Reliability and Design Life in Design of Long-span Cable-supported Bridges. *IABSE Symp. Rep.* **2014**, *102*, 64–70.
25. Wen, Y.K. Reliability and performance-based design. *Struct. Saf.* **2001**, *23*, 407–428. [CrossRef]
26. Katade, R.; Katsuki, S. Target reliability index determination method based on burden risk concept. *Doboku Gakkai Ronbunshuu A* **2009**, *65*, 42–60. [CrossRef]
27. Huaco, D.R.; Bowders, J.J.; Loehr, J.E. Transportation Research Board. Method to develop target levels of reliability for design using LRFD. In Proceedings of the 91th Annual Meeting, Washington, DC, USA, 22–26 January 2012.
28. Holicky, M. Optimum reliability level for structures. In *Vulnerability, Uncertainty, and Risk: Quantification, Mitigation, and Management, Proceedings of the Second International Conference on Vulnerability and Risk Analysis and Management (ICVRAM) and the Sixth International Symposium on Uncertainty, Modeling, and Analysis (ISUMA), Liverpool, UK, 13–16 July 2014*; American Society of Civil Engineers: Reston, VA, USA, 2014; pp. 184–193.
29. Yanaka, M.; Nowak, A.S.; Ghasemi, S.H. Reliability-based and life-cycle-cost oriented design recommendations for prestressed concrete bridge girders. *Struct. Concr.* **2016**, *17*, 836–847. [CrossRef]
30. Ghasemi, S.H.; Nowak, A.S. Target reliability for bridges with consideration of ultimate limit state. *Eng. Struct.* **2017**, *152*, 226–237. [CrossRef]
31. Sunyong Kim, B.G.; Dan, M.F. Optimum Target Reliability Determination for Efficient Service Life Management of Bridge Networks. *J. Bridge Eng.* **2020**, *25*, 04020087.
32. Nguyena, V.; Jeonga, M.C.; Hanb, T.S.; Konga, J.S. Reliability-based optimisation design of post-tensioned concrete box girder bridges considering pitting corrosion attack. *Struct. Infrastruct. Eng.* **2013**, *9*, 78–96. [CrossRef]
33. *GB/T50283-1999*; Unified Standard for Structural Reliability Design of Highway Engineering. People's Communications Press: Beijing, China, 1999.
34. *JTGD60—2015*; Common Specifications for Highway Bridges and Culverts Design. People's Communications Press: Beijing, China, 2015.
35. Darmawan, M.S.; Stewart, M.G. Spatial time-dependent reliability analysis of corroding pretensioned prestressed concrete bridge girders. *Struct. Saf.* **2007**, *29*, 16–31. [CrossRef]
36. Enright, M.P.; Dan, M.F. Probabilistic analysis of resistance degradation of reinforced concrete bridge beams under corrosion. *Eng. Struct.* **1998**, *20*, 960–971. [CrossRef]
37. Ahammed, M.; Melchers, R.E. A convenient approach for estimating time-dependent structural reliability in the load space. *Probabilistic Eng. Mech.* **2009**, *24*, 467–472. [CrossRef]
38. Li, Q.; Wang, C.; Ellingwood, B.R. Time-dependent reliability of aging structures in the presence of non-stationary loads and degradation. *Struct. Saf.* **2015**, *52*, 132–141. [CrossRef]
39. Wang, C.; Li, Q.; Ellingwood, B.R. Time-dependent reliability of ageing structures: An approximate approach. *Struct. Infrastruct. Eng.* **2016**, *12*, 1566–1572. [CrossRef]
40. Melchers, R.E. Progress in developing realistic corrosion models. *Struct. Infrastruct. Eng.* **2018**, *14*, 843–854. [CrossRef]
41. Melchers, R.E.; Chaves, I.A. A comparative study of chlorides and longer-term reinforcement corrosion. *Mater. Corros. -Werkst. Und Korros.* **2017**, *68*, 613–621. [CrossRef]
42. Bocchini, P.; Saydam, D.; Frangopol, D.M. Efficient, accurate, and simple Markov chain model for the life-cycle analysis of bridge groups. *Struct. Saf.* **2013**, *40*, 51–64. [CrossRef]
43. Guo, T.; Frangopol, D.M.; Chen, Y. Fatigue reliability assessment of steel bridge details integrating weigh-in-motion data and probabilistic finite element analysis. *Comput. Struct.* **2012**, *112*, 245–257. [CrossRef]
44. Kim, S.; Frangopol, D.M.; Soliman, M. Generalized Probabilistic Framework for Optimum Inspection and Maintenance Planning. *J. Struct. Eng.* **2013**, *139*, 435–447. [CrossRef]
45. García-Segura, T.; Yepes, V.; Frangopol, D.M.; Yang, D.Y. Lifetime reliability-based optimization of post-tensioned box-girder bridges. *Eng. Struct.* **2017**, *145*, 381–391. [CrossRef]

46. Lim, S.; Akiyama, M.; Frangopol, D.M. Assessment of the structural performance of corrosion-affected RC members based on experimental study and probabilistic modeling. *Eng. Struct.* **2016**, *127*, 189–205. [CrossRef]
47. Otsuka, H.; Furukawa, A.; Suzuki, Y.; Betsumiya, T. Reliability analysis of cable-stayed bridge considering uncertain structural properties and input ground motion. *Doboku Gakkai Ronbunshuu A* **2010**, *28*, 16.
48. Sarja, A.; Vesikari, E. Durability Design of Concrete Structures. *Mater. Struct.* **1996**, *33*, 14–20. [CrossRef]
49. Jiang, J.; Yuan, Y. Prediction model for the time-varying corrosion rate of rebar based on micro-environment in concrete. *Constr. Build. Mater.* **2012**, *35*, 625–632. [CrossRef]
50. Revert, A.B.; Weerdt, K.D.; Hornbostel, K.; Geiker, M.R. Carbonation-induced corrosion: Investigation of the corrosion onset. *Constr. Build. Mater.* **2018**, *162*, 847–856. [CrossRef]
51. Torbati-Sarraf, H.; Poursaee, A. Corrosion of coupled steels with different microstructures in concrete environment. *Constr. Build. Mater.* **2018**, *167*, 680–687. [CrossRef]
52. Chang, C.F.; Chen, J.W. The experimental investigation of concrete carbonation depth. *Cem. Concr. Res.* **2006**, *36*, 1760–1767. [CrossRef]
53. Jones, M.R.; Dhir, R.K.; Newlands, M.D.; Abbas, A.M.O. A study of the CEN test method for measurement of the carbonation depth of hardened concrete. *Mater. Struct.* **2000**, *33*, 135–142. [CrossRef]
54. Schneider, J. Some thoughts on the reliability assessment of existing structures. *Struct. Eng. Int.* **1992**, *2*, 13–18. [CrossRef]
55. Yuan, Y.; Ji, Y. Modeling corroded section configuration of steel bar in concrete structure. *Constr. Build. Mater.* **2009**, *23*, 2461–2466. [CrossRef]
56. Melchers, R.E. *Structural Reliability Analysis and Prediction*, 3rd ed.; John Wiley: Hoboken, NJ, USA, 1999.